Published in final edited form as:
Hepatology. 2010 August ; 52(2): 590–601. doi:10.1002/hep.23739.

Endothelial cell Toll-like receptor 4 regulates fibrosis associated angiogenesis in liver

K Jagavelu[*], **C Routray**[*], **U Shergill**, **SP O'Hara**, **W Faubion**, and **VH Shah**
GI Research Unit and Fiterman Center for Digestive Diseases, Mayo Clinic, Rochester, MN 55905, USA

Abstract

Angiogenesis defines the growth of new blood vessels from pre-existing vascular endothelial networks and corresponds with the wound healing process that is typified by the process of liver fibrosis. Liver fibrosis is also associated with increased endotoxin within the gut lumen and its associated portal circulation. However, the interrelationship of gut endotoxin and its receptor, Toll-like receptor 4 (TLR4), with liver fibrosis and associated angiogenesis remains incompletely defined.

RESULT—Here we provide evidence, using complementary genetic, molecular, and pharmacologic approaches that the pattern recognition receptor that recognizes endotoxin, TLR4, expressed on liver endothelial cells (LEC), regulates angiogenic responses both *in vitro* and *in vivo*. Mechanistic studies reveal a key role for a cognate TLR4 effector protein, MyD88 in this process which culminates in extracellular protease production that regulates LEC invasive capacity, a key step in angiogenesis. Furthermore TLR4 dependent angiogenesis *in vivo* corresponds with fibrosis in complementary liver models of fibrosis.

CONCLUSION—These studies provide evidence that the TLR4 pathway in LEC regulates angiogenesis through its MyD88 effector protein by regulating extracellular protease production and that this process is linked to the development of liver fibrosis.

Keywords

Endotoxin; MyD88; Portal hypertension; Lipopolysaccharide

Introduction

Angiogenesis, the sprouting of new vessels from pre-existing ones, is an essential physiological process required for embryogenesis, growth, regeneration and wound healing (1). In liver cirrhosis, an exuberant wound healing response to liver injury culminates in fibrosis, angiogenesis, and vascular reorganization (2). However, the precise relationship between fibrosis, angiogenesis, and vascular reorganization has remained enigmatic.

Toll like receptors (TLRs) belong to a class of pattern recognition receptors and bind molecules broadly shared by pathogens collectively referred to as pathogen-associated molecular patterns (3,4). At least ten mammalian TLRs have been cloned, each recognizing a specific molecular product derived from major classes of pathogens (5). From within this family of TLR proteins, TLR4 recognizes lipopolysaccharide (LPS), a Gram-negative

Corresponding Author: Vijay Shah, M.D., Phone: 507-255-6028, shah.vijay@mayo.edu.
[*]These authors contributed equally to this work.

bacterial cell-wall component that is enriched within the intestinal lumen and its associated portal circulation (6).

TLR4 maintains capabilities to signal through the adapter molecule, MyD88, as well as through a MyD88-independent pathway (7). In the canonical TLR4-MyD88 pathway, binding of TLR4 by LPS activates MyD88 through its cytosolic domain, which further triggers a cascade of intracellular signaling events leading to activation of NF-kB and inflammation (4). Conversely, TLR4 can stimulate the expression of interferon-β (IFN-β) in a MyD88-independent fashion involving toll-like receptor adaptor molecule (TRAM or TIRP) (8). Other non-canonical pathways have also been recently identified (9). Nonetheless, some recent reports suggest that in vascular endothelial cells, TLR4 signals may channel preferentially through MyD88 (10).

Prior studies associate portal venous LPS with cirrhosis, suggesting a possible direct effect of LPS on Kupffer cells and hepatic stellate cells (11,12). However, liver endothelial cells (LEC), are the first line of cells exposed to portal venous LPS. These cells also mediate sinusoidal remodeling and angiogenesis, processes that accompany liver fibrosis. These observations make a potential role of LPS on LEC signaling, a compelling scenario.

Based on these concepts, we hypothesize that TLR4 signaling within LEC contribute to angiogenesis, sinusoidal remodeling, and cirrhosis. In support of this hypothesis, we demonstrate TLR4 expression and function in LEC leading to angiogenesis *in vitro*. Mechanistically, this effect is achieved by virtue of the TLR4 effector protein, Myd88 and culminates in secretion of the extracellular protease, MMP2 that promotes LEC invasion. Furthermore, angiogenesis and fibrosis are concurrently attenuated in TLR4 deficient mice. Lastly, we provide direct *in vivo* evidence that TLR4 mediates angiogenesis in complementary models of angiogenesis. Thus, these multidisciplinary studies expand our understanding of angiogenesis, its relationship to fibrosis, and concurrently identify a new function for pattern recognition receptors in endothelial cells.

Methods

Animals

C3H/HeOuJ (TLR4-WT) and C3H/HeJ (TLR4-MT), which carry a spontaneous mutation, that confers a loss of TLR4 function, were purchased from Jackson Laboratories (Bar Harbor ME). These animals have similar levels of TNF-α under basal conditions but impaired production in response to LPS (13). Bile duct ligation (BDL) and sham surgeries were performed as previously described (14). For CCl_4 induced fibrosis studies, administration of carbon tetrachloride (CCl_4; 1 mg/kg body weight) or vehicle (olive oil) was injected intraperitoneally for a period of six weeks as previously described (15). LEC were isolated from mice as previously described (16,17) and purity was assessed. All procedures were approved by Mayo Clinic Institutional Animal Care and Use Committee (IACUC).

Cell culture and transfection

Human LEC (ScienCell, San Diego, CA) were grown in standard tissue culture conditions (a humidified, 37°C, 5% CO_2 incubator) in media containing 5% fetal bovine serum, 2% endothelial cell growth supplement and 1% penicillin/streptomycin (ScienCell, San Diego, CA). Retroviral transduction and siRNA transfection were performed as we previously described (18). Two distinct siRNAs for TLR4 within the coding region starting at 105 and 174bp and MyD88 was a gift from Steven O'Hara while TRAM siRNA was commercially obtained (Thermo Scientific). Human MyD88 full length and dominant negative N-terminal truncation mutant constructs were PCR amplified from pUNO-hMyD88 and pDeNy-

hMyD88 (Invivogen) respectively, and the amplified fragments were sub-cloned into the pMMP retroviral vector.

In vitro tubulogenesis

Murine and human LEC transduced with MyD88 or YFP retrovirus, or preincubated with a MyD88 dimerization inhibitor (19) (Imgenex) for 24 hrs were cultured in endothelial cell medium, before plating in 4 well coated chamber slides (2×10^4 cells per well) pre-coated with 70 μL Matrigel (growth factor-reduced; BD Biosciences, San Jose, CA). Tubulogenesis was visualized using an inverted microscope (Zeiss Axiovert 40 CFL, 4× magnification), captured with a CCD digital camera (Jenoptix, Jena, Germany), after 3 or 6 hours of culturing in the presence of either vehicle or 1 μg/ml LPS (13,20) at 37 °C and 5% CO_2, and quantified using Image Pro Software as previously described (15). Cell viability was measured using Calcein AM (Invitrogen).

Matrigel plug assay

Anesthetized TLR4-WT and TLR4-MT mice, received 300 μl injections of sterile Matrigel (growth factor reduced; BD Biosciences (Cat. No 356231) (21) and VEGF (50 ng/mL; R&D systems, Minneapolis) into the subcutaneous layer in two locations. Matrigel plugs were removed 14 days after implantation, photographed, and divided into 2 blocks. One Matrigel plug was allowed to liquify at 4° C, and hemoglobin content was determined by the Drabkin method according to the manufacturer's protocol (Sigma, St. Louis, MO). Absorbance was measured at 540 nm and hemoglobin concentration was calculated and normalized to the plug weight. The other Matrigel block was fixed overnight in formalin and embedded in paraffin. Sections (6 μm) were stained with hematoxylin and eosin (H&E) and were visualized by traditional light microscopy.

Immunoblotting

Proteins from cellular extracts were subjected to denaturing 12% SDS-polyacrylamide gels and transferred to nitrocellulose membranes. After blocking, the blots were probed with anti-TLR4 (1:1000) and anti-MyD88 (1:1000) (Imgenex). The blots were washed and incubated for one hour at room temperature with appropriate horseradish peroxidase-conjugated secondary antibodies. Protein bands were detected using an enhanced chemiluminescence detection system (ECL Plus, Santa Cruz). After exposing the nitrocellulose sheets to Kodak XAR film, the autoradiographs were scanned. Equal protein loading was verified by re-probing the membrane with an anti-β-actin antibody (1:5000).

Confocal Immunofluorescence microscopy

For immunostaining, murine and human LEC were cultured to ~50% confluence on gelatin-coated cover slips in 24-well plates. Frozen liver sections from sham, BDL, olive oil, or CCl_4 treated TLR4-WT and TLR4-MT mice were fixed with ice-cold acetone and were blocked with 10% goat serum for 2 hours at room temperature to eliminate nonspecific background signals. Cells or tissues sections were then incubated with antibodies against TLR4 (Sigma) (each 1:400), vWF (Sigma) (1:400), F4/80 (Abcam) (1:150), CD11b (Abcam) (1:200), Aquaporin-1 (Alpha Diagnostics Intl.; (1:500) (Recent studies show that aquaporin-1 stains liver endothelial cells including cirrhotic neo-vessels (22)) and PDGFRβ (Cell Signalling) (1:100) at 4° C overnight followed by incubation with appropriate fluorescein isothiocyanate (FITC) or Alexa Fluor 568 conjugated secondary antibodies (Invitrogen) for 1 hour at room temperature. Nuclei were counterstained with TOTO-3 stain. Immunofluorescent staining was visualized using a confocal microscope (Zeiss LSM Pascal Axiovert; Carl Zeiss Ltd.) and images from vWF and Aquaporin-1 staining were quantified

using Metamorph Software (version 7.6, Molecular Devices, USA). Fibrosis quantification was carried out from Sirius red stained sections.

Aortic Ring Assay

Aortas were excised from thoracic region from 8-week-old male TLR4-WT or TLR4-MT mice and immediately placed in ice cold PBS. The fat tissue was removed atraumatically and aortus were subsequently cut into 0.3 mm rings using a dissecting microscope. The rings were then placed in 100 μl of Matrigel (growth factor reduced; BD Biosciences (Cat. No 356231) and incubated at 37°C in a humidified 5% CO2 incubator for gelation. Rings were incubated in media with varying compounds as indicated in specific experiments. The plates were incubated in 37°C in a humidified 5% CO2 incubator for 7 days. The rings were fixed in 4% formaldehyde, photographs of rings were captured using a phase contrast microscope (Zeiss, 10× magnification), and captured with a CCD camera (Jenoptix). Morphometric analysis of sprouting specifically within the vessel ring lumen was quantified using Image Pro Software (Bethesda, MD).

Quantitative RT-PCR

Total RNA was extracted from human and mouse LEC using Trizol (Invitrogen) and cDNA synthesis was performed from 1μg of total RNA using SuperScript III (Invitrogen). Real-time amplification was carried out with Applied Biosystems 7500 detection systems. Species specific primers were designed and utilized (sequences available on request). TLR-4 mRNA levels were normalized to β-actin mRNA and shown as fold change.

Transwell collagen invasion assay

LEC invasion was studied using 3D collagen assay as previously described (23). Polycarbonate membrane transwell inserts (8 μm pore size) (Corning, USA) were coated with Collagen type I (50 μg/μl). Primary LEC from TLR4-WT or TLR4-MT mice were plated on to the membrane of the transwell insert (40,000 cells/well) on top of a thick layer of type-I collagen (3 mg/ml). The lower chambers were filled with serum free medium containing 10 ng/ml of mouse VEGF or FGF or vehicle (22,24). Transwell inserts were removed after 24 hours of incubation, fixed, stained with DAPI and quantified using Metamorph Software (version 7.6, Molecular Devices, USA).

Gelatin Zymography

Murine LEC isolates were lysed and separated by 10% SDS PAGE impregnated with 1mg/ml gelatin. The gel was then renatured for 30 min in 2.5% Triton X-100 and subsequently incubated for 24 hours at 37° C in substrate buffer incubation (50 mmol/L Tris/HCl, pH 7.5, containing 5 mmol/L $CaCl_2$, 0.02% Brij-35) for MMP degradation of gelatin. Gels were stained with 0.5% Coomassie blue. Quantification of gelatinolytic areas was measured using Image-J (Bethesda, MD).

In situ zymography

Frozen liver sections from TLR4-WT and TLR4-MT mice were incubated on 1% agarose fortified with fluorescent gelatin (Molecular Probes, Invitrogen). The sections were then incubated at 37° C in substrate development buffer and EDTA was used as negative control as previously described (25).

Proliferation Assay

Primary LEC were cultured for 24 and 48 hrs and subsequently incubated with MTS reagent (Promega, Madison USA). The absorbance of the plate was read colorimetrically at OD 490

nm. Standardization and other steps were performed according to manufacturer's instructions.

Statistical Analysis

Data are expressed as mean±SEM of at least three independent experiments. Groups were compared by a two-tailed Student's T-test. A P-value of less than 0.05 was considered as statistically significant.

Results

Expression of TLR4 in human and murine LEC

As a first step to explore a role for TLR4 in liver fibrosis-associated angiogenesis, we determined the expression of TLR4 in LEC from both humans and mice. Confirmatory of prior studies (26), qRT-PCR analysis detected TLR4 mRNA levels in both human and murine LEC**,** with levels being substantially elevated compared to other systemic human endothelial cells such as human umbilical vein endothelial cells (HUVECS), though less than the lymphocyte positive control Raji cells (Fig. 1A). This observation was substantiated by detection of a specific immunofluorescence signal for TLR4 in isolated mouse and human LEC (Fig. 1B) indicating that TLR4 is expressed on both murine and human LEC. Although other TLR molecules were also expressed within LEC (data not shown), they were not pursued in further detail at this time. Rather, the present studies were focused in a hypothesis based manner on the LPS recognizing TLR4 and its potential relevance to liver injury, fibrosis and vascular integrity, owing to the proposed links of LPS with these processes.

TLR4 promotes LEC driven angiogenesis in vitro

Reorganization of endothelial cells into tube-like vascular structures in Matrigel, referred to as tubulogenesis, provides an *in vitro* estimation of the angiogenic capacity of vascular cells since a number of steps required for angiogenesis *in vivo* are required for tubulogenesis *in vitro* (15). To test TLR4 functional relevance in angiogenesis, we isolated LEC from TLR4-MT or TLR4 WT mice and measured tubulogenesis. As seen in Figs. 2A and B, while LPS prominently stimulated tubulogenesis in WT mice, both basal and LPS-stimulated tubulogenesis were markedly attenuated in TLR4-MT mice. The antibiotic polymyxin-B, inhibited tubulogenesis in all groups which further supported the role of basal LPS and TLR4 in this process.

To study the functional relevance of TLR4 in human cells, we next performed corroborative studies using TLR4 siRNA. The increased tubulogenesis of human LEC in response to LPS is demonstrated in Fig. 2B. Transfection of TLR4 siRNA into human LEC significantly inhibited basal tubulogenesis as compared to transfection of a scrambled siRNA control (Figs. 2C and D, $p<0.05$; inset Western blot depicts siRNA knockdown of the doublet TLR4 protein band as previously described (27)). Additionally, reduction in tubulogenesis was not due to cell toxicity as assessed by staining of cells in Matrigel with the cell viability dye Calcein, AM (Supplementary Figs. 2A and B). Similar results were also obtained with a second TLR4 siRNA recognizing a distinctly different region of human TLR4 mRNA (Fig. 2C). In these and ensuing *in vitro* experiments of tubulogenesis conducted on Matrigel, we observed prominent effects of experimental interventions on basal responses in absence of LPS, likely due to endogenous TLR4 ligands that are present within matrix rich environments such as Matrigel (28-30) and therefore data are depicted as basal responses to Matrigel rather than by addition of exogenous LPS. These complementary genetic and molecular approaches provide evidence that TLR4 promotes angiogenesis in LEC *in vitro*.

MyD88 is responsible for TLR4 driven tubulogenesis

TLR4 signaling in response to LPS may occur by a MyD88 dependent or a MyD88 independent, TRAM dependent pathway (6). To identify the pathway which mediates the angiogenic signals of TLR4, we overexpressed MyD88 using a retroviral construct in human LEC. MyD88 overexpression in human LEC significantly enhanced tubulogenesis as compared to cells transduced with a control retrovirus (Fig. 3A). To confirm specificity, we transfected human LEC with MyD88 siRNA or control siRNA. Basal tubulogenesis was reduced in LEC transfected with MyD88 siRNA as compared to control siRNA ($P<0.05$; Fig. 3B), in absence of siRNA-induced cell toxicity (Supplementary Figs. 2C and D). To further confirm whether TLR4 dependent angiogenesis occurs through MyD88 function, we blocked MyD88 homodimerization using the peptide IMG-2005-1, thus blocking MyD88 function (19). The MyD88 inhibitory peptide attenuated tubulogenesis in human LEC compared to a vehicle control peptide (Fig. 3C). Furthermore, overexpression of a dominant-negative, N-terminal truncated form of MyD88 also significantly reduced tubulogenesis (Fig. 3D). To further link TLR4 signals through MyD88, we silenced MyD88 in human LEC and returned to the LPS stimulation model. Indeed, silencing of MyD88 reduced LPS mediated tube formation compared to control siRNA, suggesting that angiogenic signaling in these cells requires MyD88 activation downstream of TLR4 (Fig. 3E). Conversely, a small and not statistically significant difference in tubulogenesis was observed by silencing TRAM using siRNA (Supplementary Fig. 3). In total, these studies using multiple complementary approaches indicate that TLR4-dependent tubulogenesis is mediated through MyD88.

Matrigel invasive capacity is reduced in TLR4-MT endothelial cells

The ability of endothelial cells to invade through matrix is a key cellular step involved in angiogenesis especially in the cirrhotic microenvironment (31). We were especially interested in potential effects of TLR4 on matrix regulatory proteins relevant for invasion since our initial hypothesis generating, focused microarray analyses (Endothelial Cell Superarray; SA Bioscience) comparing gene expression profiles of TLR4-WT and TLR4-MT LEC revealed prominent differences in expression levels of several MMPs and TIMPs (Supplementary Fig. 5A). To determine whether TLR4 regulates the matrix invasive capacity of LEC, primary murine LEC were plated on transwell chambers, coated with collagen and cell invasion was measured. TLR4-MT LEC evidenced reduced invasion (Figs. 4A and B) in response to VEGF or FGF, compared to TLR4-WT LEC. However, no significant difference in proliferation of primary LEC isolated from TLR4-WT or TLR4-MT mice at 24 and 48 hours was observed by MTS proliferation assay providing a relevant control (Supplementary Fig. 4). To assess the mechanism by which TLR4 may regulate LEC invasion, we measured the levels of MMP-2, a key extracellular protease that promotes cell invasion and is highly relevant to cirrhosis (32), by gelatin zymography. Indeed, both active and pro forms of MMP-2 were reduced in both cell lysates and supernatants of TLR4-MT LEC compared to the TLR4-WT (Figs. 4C and D; duplicate samples are depicted). Furthermore, TLR4-MT mouse liver evidenced reduced gelatinase activity compared to TLR4-WT mice as assessed by in situ gelatin zymography (Supplementary Fig. 5B), consistent with prior studies showing that TLR4 regulates MMP production (33). These results suggest that reduced angiogenesis observed in TLR-MT LEC may be due to reduced MMP2 dependent invasive capacity.

Angiogenesis is reduced in TLR4-MT mice in intact tissues and in vivo

Next, to directly determine if TLR4 regulates angiogenesis *in vivo*; we subcutaneously injected Matrigel into TLR4-WT and TLR4-MT mice. TLR4-MT mice showed significantly reduced neovascularization compared to TLR4-WT both grossly and histologically (Figs. 5A and B). To further confirm reduced neovascularization, we quantified the hemoglobin

content of the matrigel plug which was also significantly reduced in TLR4-MT mice compared to TLR4-WT (Fig. 5C). These results were also extended to an additional model of angiogenesis; the aortic ring assay in which aorta from TLR4-WT and TLR4-MT mice were sectioned and cultured *in vitro*. Vascular sprout formation from the rings was measured as a parameter of angiogenic potential (34). In line with the prior vascular analyses, aortic rings derived from TLR4-MT mutant mice showed less sprouting when stimulated with LPS, compared to wild type aortic rings (Fig. 5D), further corroborating an angiogenic role of endothelial cell TLR4.

TLR4 deletion shows parallel effects on both liver fibrosis and liver angiogenesis

We next sought to examine the role of TLR4 in the angiogenic response that is associated with fibrosis using two distinct models of liver injury and fibrosis (35). First, BDL was performed in TLR4-WT and TLR4-MT mice which were sacrificed after 3 weeks. Histological analysis revealed reduced fibrosis in TLR4-MT mice compared to TLR4-WT mice (Figs. 6A and B; Sirius red and H&E, respectively), consistent with data that was recently published (11). More detailed analysis of the hepatic vasculature revealed that vWF positive endothelial cell density was markedly increased in TLR4-WT mice after BDL in a manner that corresponded with the degree of liver fibrosis (Figs. 6 C and D). Corroborative results were obtained with an additional endothelial cell marker, aquaporin-1 (22) (Supplementary Fig. 6). Furthermore, the diminished fibrosis that was observed in BDL TLR4-MT mice corresponded with diminished vascular density in these mice. Concordant results were also observed in TLR4-WT and TLR4-MT mice undergoing analysis after CCl_4 induced liver fibrosis, further substantiating the role of LEC TLR4 in fibrosis-associated angiogenesis (Fig. 7; Panels A and B depict fibrosis as assessed by Sirius red stain, Panels C and D depict vascular density based on vWF positive endothelial cell staining, and Supplementary Fig. 6., Panels C and D depict aquaporin-1 positive vascular density in CCl_4 mice).

Discussion

Since gut derived LPS traverses directly into liver via portal vein, effects of the TLR4 pathway in liver function and pathobiology are an emerging area of interest. In turn, changes in vascular function and structure are increasingly recognized to be closely linked with liver injury and fibrosis (36). Our present work makes a number of important observations that link TLR4 with angiogenesis and liver fibrosis. Specifically, our study provides the following new findings: 1) TLR4 is expressed in LEC and contributes to cirrhosis-associated angiogenesis in liver, 2) TLR4 angiogenic signaling in LEC occurs through the MyD88 dependent pathway, 3) TLR4 angiogenesis is associated with MMP2-mediated LEC matrix invasion, and 4) inhibition of TLR4 inhibits angiogenesis in parallel with fibrosis in murine models of liver injury and cirrhosis, providing an important link between two processes.

TLR4 are pattern recognition molecules which detect specific proteins derived from bacteria, viruses and fungi, thereby playing a key role in innate immunity (37). TLR4 in particular detects LPS from the cell wall of gram negative bacteria (38). While most extensively studied in traditional blood immune cells, LPS binding to the endothelial cell surface may regulate endothelial cell immune function through the TLR4-MD2-CD14 complex (39-41). Our study adds to the current paradigms of TLR4 function in endothelial cells by revealing that TLR4 induced activation of LEC leads to angiogenesis. Indeed, LEC from TLR4 mutant mice revealed prominent defects in angiogenic function as revealed by a number of complementary *in vivo* and *in vitro* assays including tubulogenesis, aortic sprouting, and matrigel plug assay. Since MyD88 is an essential adaptor protein for TLR4 signaling, we postulated that TLR4 angiogenic signals may transduce through MyD88. Indeed, overexpression of MyD88 in LEC increased tubulogenesis while inhibition of this

pathway by siRNA based silencing, dominant negative perturbation, and small molecule inhibition blocked angiogenic signals. However, some of the quantitative differences in tubulogenesis that we observed in response to inhibition of the two pathways suggest that other non-canonical pathways could also be contributing (9). Thus, our work mechanistically builds on prior work pertaining to LPS and LEC function (42) and also identifies links to cirrhosis pathobiology with mechanistic insights as further outlined below.

VEGF expression is increased in cirrhotic liver (43,44) and furthermore, there is increased vascular endothelial proliferation and vascular density in both human and murine cirrhosis (35,45). Indeed, it has been postulated that active angiogenesis may perpetuate the fibrosis process through multiple potential mechanisms (46). In the BDL model, ligation of the bile duct causes portal hypertension and mesenteric congestion which may promote translocation of LPS from intestinal microflora to the hepatic sinusoids across the gut barrier. Thus, we postulate that this endotoxic load may activate TLR4 in liver SEC and thereby promote angiogenesis in conjunction with fibrosis. Indeed, we observed significant histologic changes in TLR4-MT mice after BDL compared to the wild type and sham operated controls, with immunohistochemistry revealing not only less fibrosis but also less neovascularization. Since concordant results were obtained in the mechanistically distinct CCl_4 model, these observations in total suggest that TLR4 signaling in liver EC may provide a requisite link between hepatic neovascularization and fibrogenesis. Indeed, this observation is of particular interest in the context of recent studies identifying that TLR4 in hepatic stellate cells is a key driver of the fibrosis process (11). Studies requiring generation and utilization of mice with targeted deletion of TLR4 exclusively in LEC, Kupffer cells, or hepatic stellate cells will be required to elaborate further on the specific contribution of LEC-TLR4 to the liver fibrosis process.

EC invasion and matrix degradation are a prerequisite for angiogenesis (47). In the 3D collagen invasion assay, we found reduced invasive capacity of TLR4-MT LEC, which was attributed to reduced MMP-2 production. While matrix constituents clearly influence sinusoidal cell behavior (11,28,48), precisely how EC sense the changes in matrix in their microenvironment is not well understood (49). Since some studies suggest that TLR4 binds specific fibronectin splice variants, hyaluronan and other matrix components (28-30) in addition to its canonical LPS binding capacity, it is tempting to speculate that TLR4 may act as an EC-sensor of the matrix microenvironment and thereby regulate EC production of MMP-2 and subsequent EC invasion and angiogenesis (33). This concept is supported by TLR4 activation in LEC that was observed in response to Matrigel which contains a broad array of matrix proteins and constituents. However, further studies are required to ascertain the precise role of EC TLR4 in the process of matrix sensing.

Activation of TLR4 leads to the downstream activation of the canonical NF-kB inflammatory pathway (50). Indeed, inflammatory cell infiltration is often linked with angiogenesis as a secondary phenomenon owing to release of angiogenic substances by infiltrating inflammatory cells (51). Thus, a question that emerges from our observations is whether TLR induced angiogenesis is driven by direct EC signaling or rather if angiogenesis is a secondary phenomenon that is pursuant to TLR induced inflammatory cell infiltration. These directions will be of interest especially in context of cirrhosis whereby TLR4 function in nearly every liver cell type may be contributing to the fibrosis phenotype.

In summary, the present studies make several new observations that identify innate immune pathways in the process of angiogenesis and its relationship with liver fibrosis. Future studies will be needed to further dissect the precise roles of TLR4 on different hepatic cell populations and their convergent effects on liver fibrosis and its associated changes in vascular structure and integrity.

Supplementary Material

Refer to Web version on PubMed Central for supplementary material.

Acknowledgments

The authors acknowledge Tim Billiar for helpful discussions, Helen Hendrickson for excellent technical support and Theresa Johnson for secretarial support.

Financial Support: This work was supported by the grants from NIH R01 DK 59615 and R01 HL 86990 (V.H.S.) and P30 DK 084567 – Clinical Core.

References

1. Kim KJ, Li B, Winer J, Armanini M, Gillett N, Phillips HS, Ferrara N. Inhibition of vascular endothelial growth factor-induced angiogenesis suppresses tumour growth in vivo. Nature 1993;362:841–844. [PubMed: 7683111]
2. Lee JS, Semela D, Iredale J, Shah VH. Sinusoidal remodeling and angiogenesis: a new function for the liver-specific pericyte? Hepatology 2007;45:817–825. [PubMed: 17326208]
3. Takeda K, Akira S. Toll-like receptors in innate immunity. Int Immunol 2005;17:1–14. [PubMed: 15585605]
4. O'Neill LA. The interleukin-1 receptor/Toll-like receptor superfamily: 10 years of progress. Immunol Rev 2008;226:10–18. [PubMed: 19161412]
5. Akira S. Toll-like receptors and innate immunity. Adv Immunol 2001;78:1–56. [PubMed: 11432202]
6. Szabo G, Dolganiuc A, Mandrekar P. Pattern recognition receptors: a contemporary view on liver diseases. Hepatology 2006;44:287–298. [PubMed: 16871558]
7. Kaisho T, Takeuchi O, Kawai T, Hoshino K, Akira S. Endotoxin-induced maturation of MyD88-deficient dendritic cells. J Immunol 2001;166:5688–5694. [PubMed: 11313410]
8. Yamamoto M, Sato S, Hemmi H, Uematsu S, Hoshino K, Kaisho T, Takeuchi O, et al. TRAM is specifically involved in the Toll-like receptor 4-mediated MyD88-independent signaling pathway. Nat Immunol 2003;4:1144–1150. [PubMed: 14556004]
9. Choi SH, Harkewicz R, Lee JH, Boullier A, Almazan F, Li AC, Witztum JL, et al. Lipoprotein accumulation in macrophages via toll-like receptor-4-dependent fluid phase uptake. Circ Res 2009;104:1355–1363. [PubMed: 19461045]
10. Harari OA, Alcaide P, Ahl D, Luscinskas FW, Liao JK. Absence of TRAM restricts Toll-like receptor 4 signaling in vascular endothelial cells to the MyD88 pathway. Circ Res 2006;98:1134–1140. [PubMed: 16574902]
11. Seki E, De Minicis S, Osterreicher CH, Kluwe J, Osawa Y, Brenner DA, Schwabe RF. TLR4 enhances TGF-beta signaling and hepatic fibrosis. Nat Med 2007;13:1324–1332. [PubMed: 17952090]
12. Roychowdhury S, McMullen MR, Pritchard MT, Hise AG, van Rooijen N, Medof ME, Stavitsky AB, et al. An early complement-dependent and TLR-4-independent phase in the pathogenesis of ethanol-induced liver injury in mice. Hepatology 2009;49:1326–1334. [PubMed: 19133650]
13. Hoshino K, Takeuchi O, Kawai T, Sanjo H, Ogawa T, Takeda Y, Takeda K, et al. Cutting edge: Toll-like receptor 4 (TLR4)-deficient mice are hyporesponsive to lipopolysaccharide: evidence for TLR4 as the Lps gene product. J Immunol 1999;162:3749–3752. [PubMed: 10201887]
14. Shah V, Hendrickson H, Cao S, Yao J, Katusic Z. Regulation of hepatic endothelial nitric oxide synthase by caveolin and calmodulin after bile duct ligation in rats. Am J Physiol 2001;280:G1209–1216.
15. Semela D, Das A, Langer DA, Kang N, Leof E, Shah VH. Platelet-derived growth factor signaling through ephrin-B2 regulates hepatic vascular structure and function. Gastroenterology 2008;135:671–679. [PubMed: 18570897]
16. Zirlik A, Bavendiek U, Libby P, MacFarlane L, Gerdes N, Jagielska J, Ernst S, et al. TRAF-1, -2, -3, -5, and -6 are induced in atherosclerotic plaques and differentially mediate proinflammatory

functions of CD40L in endothelial cells. Arterioscler Thromb Vasc Biol 2007;27:1101–1107. [PubMed: 17332487]

17. LeCouter J, Moritz DR, Li B, Phillips GL, Liang XH, Gerber HP, Hillan KJ, et al. Angiogenesis-independent endothelial protection of liver: role of VEGFR-1. Science 2003;299:890–893. [PubMed: 12574630]
18. Kang-Decker N, Chatterjee S, Yao J, Egan J, Semela D, Mukhopadhyay D, Shah V. Nitric oxide promotes endothelial cell survival signaling through S-nitrosylation and activation of dynamin-2. J Cell Sci 2007;120:492–501. CS. [PubMed: 17251380]
19. Loiarro M, Sette C, Gallo G, Ciacci A, Fanto N, Mastroianni D, Carminati P, et al. Peptide-mediated interference of TIR domain dimerization in MyD88 inhibits interleukin-1-dependent activation of NF-{kappa}B. J Biol Chem 2005;280:15809–15814. [PubMed: 15755740]
20. Chen Y, Lu N, Ling Y, Gao Y, Wang L, Sun Y, Qi Q, et al. Wogonosideinhibits lipopolysaccharide-induced angiogenesis in vitro and in vivo via toll-like receptor 4 signal transduction. Toxicology 2009;259:10–17. [PubMed: 19428938]
21. Ringden O, Quadracci LJ, Groth CG. The effects of anti-lymphocyte globulin on lymphocyte subpopulations in recipients of kidney allografts. Scand J Urol Nephrol Suppl 1977:86–89. [PubMed: 356231]
22. Huebert RC, Vasdev M, Shergill U, Das A, Huang B, Charlton M, LaRusso NF, et al. Aquaporin-1 Facilitates Angiogenic Invasion in the Pathologic Neovasculature that Accompanies Cirrhosis. Hepatology. 2010 in press.
23. Decker NK, Abdelmoneim SS, Yaqoob U, Hendrickson H, Hormes J, Bentley M, Pitot H, et al. Nitric oxide regulates tumor cell cross-talk with stromal cells in the tumor microenvironment of the liver. Am J Pathol 2008;173:1002–1012. [PubMed: 18755846]
24. Jih YJ, Lien WH, Tsai WC, Yang GW, Li C, Wu LW. Distinct regulation of genes by bFGF and VEGF-A in endothelial cells. Angiogenesis 2001;4:313–321. [PubMed: 12197476]
25. Galis ZS, Sukhova GK, Libby P. Microscopic localization of active proteases by in situ zymography: detection of matrix metalloproteinase activity in vascular tissue. Faseb J 1995;9:974–980. [PubMed: 7615167]
26. Li Y, Xiang M, Yuan Y, Xiao G, Zhang J, Jiang Y, Vodovotz Y, et al. Hemorrhagic shock augments lung endothelial cell activation: role of temporal alterations of TLR4 and TLR2. Am J Physiol Regul Integr Comp Physiol 2009;297:R1670–1680. [PubMed: 19828841]
27. Zager RA, Johnson AC, Lund S, Randolph-Habecker J. Toll-like receptor (TLR4) shedding and depletion: acute proximal tubular cell responses to hypoxic and toxic injury. Am J Physiol Renal Physiol 2007;292:F304–312. [PubMed: 16885150]
28. Okamura Y, Watari M, Jerud ES, Young DW, Ishizaka ST, Rose J, Chow JC, et al. The extra domain A of fibronectin activates Toll-like receptor 4. J Biol Chem 2001;276:10229–10233. [PubMed: 11150311]
29. Jiang W, Zhang Y, Xiao L, Van Cleemput J, Ji SP, Bai G, Zhang X. Cannabinoids promote embryonic and adult hippocampus neurogenesis and produce anxiolytic- and antidepressant-like effects. J Clin Invest 2005;115:3104–3116. [PubMed: 16224541]
30. Schaefer L, Babelova A, Kiss E, Hausser HJ, Baliova M, Krzyzankova M, Marsche G, et al. The matrix component biglycan is proinflammatory and signals through Toll-like receptors 4 and 2 in macrophages. J Clin Invest 2005;115:2223–2233. [PubMed: 16025156]
31. Taura K, De Minicis S, Seki E, Hatano E, Iwaisako K, Osterreicher CH, Kodama Y, et al. Hepatic stellate cells secrete angiopoietin 1 that induces angiogenesis in liver fibrosis. Gastroenterology 2008;135:1729–1738. [PubMed: 18823985]
32. Olaso E, Ikeda K, Eng FJ, Xu L, Wang LH, Lin HC, Friedman SL. DDR2 receptor promotes MMP-2-mediated proliferation and invasion by hepatic stellate cells. J Clin Invest 2001;108:1369–1378. [PubMed: 11696582]
33. Timmers L, Sluijter JP, van Keulen JK, Hoefer IE, Nederhoff MG, Goumans MJ, Doevendans PA, et al. Toll-like receptor 4 mediates maladaptive left ventricular remodeling and impairs cardiac function after myocardial infarction. Circ Res 2008;102:257–264. [PubMed: 18007026]
34. Auerbach R, Lewis R, Shinners B, Kubai L, Akhtar N. Angiogenesis assays: a critical overview. Clin Chem 2003;49:32–40. [PubMed: 12507958]

35. Tugues S, Fernandez-Varo G, Munoz-Luque J, Ros J, Arroyo V, Rodes J, Friedman SL, et al. Antiangiogenic treatment with sunitinib ameliorates inflammatory infiltrate, fibrosis, and portal pressure in cirrhotic rats. Hepatology 2007;46:1919–1926. [PubMed: 17935226]
36. Valfre di Bonzo L, Novo E, Cannito S, Busletta C, Paternostro C, Povero D, Parola M. Angiogenesis and liver fibrogenesis. Histol Histopathol 2009;24:1323–1341. [PubMed: 19688698]
37. Takeda K, Kaisho T, Akira S. Toll-like receptors. Annu Rev Immunol 2003;21:335–376. [PubMed: 12524386]
38. Chung DW, Yoo KY, Hwang IK, Kim DW, Chung JY, Lee CH, Choi JH, et al. Systemic Administration of Lipopolysaccharide Induces Cyclooxygenase-2 Immunoreactivity in Endothelium and Increases Microglia in the Mouse Hippocampus. Cell Mol Neurobiol. 2009
39. da Silva Correia J, Soldau K, Christen U, Tobias PS, Ulevitch RJ. Lipopolysaccharide is in close proximity to each of the proteins in its membrane receptor complex. transfer from CD14 to TLR4 and MD-2. J Biol Chem 2001;276:21129–21135. [PubMed: 11274165]
40. Dauphinee SM, Karsan A. Lipopolysaccharide signaling in endothelial cells. Lab Invest 2006;86:9–22. [PubMed: 16357866]
41. Andonegui G, Zhou H, Bullard D, Kelly MM, Mullaly SC, McDonald B, Long EM, et al. Mice that exclusively express TLR4 on endothelial cells can efficiently clear a lethal systemic Gram-negative bacterial infection. J Clin Invest 2009;119:1921–1930. [PubMed: 19603547]
42. Pollet I, Opina CJ, Zimmerman C, Leong KG, Wong F, Karsan A. Bacterial lipopolysaccharide directly induces angiogenesis through TRAF6-mediated activation of NF-kappaB and c-Jun N-terminal kinase. Blood 2003;102:1740–1742. [PubMed: 12714497]
43. Corpechot C, Barbu V, Wendum D, Kinnman N, Rey C, Poupon R, Housset C, et al. Hypoxia-induced VEGF and collagen I expressions are associated with angiogenesis and fibrogenesis in experimental cirrhosis. Hepatology 2002;35:1010–1021. [PubMed: 11981751]
44. El-Assal ON, Yamanoi A, Soda Y, Yamaguchi M, Igarashi M, Yamamoto A, Nabika T, et al. Clinical significance of microvessel density and vascular endothelial growth factor expression in hepatocellular carcinoma and surrounding liver: possible involvement of vascular endothelial growth factor in the angiogenesis of cirrhotic liver. Hepatology 1998;27:1554–1562. [PubMed: 9620326]
45. Medina J, Arroyo AG, Sanchez-Madrid F, Moreno-Otero R. Angiogenesis in chronic inflammatory liver disease. Hepatology 2004;39:1185–1195. [PubMed: 15122744]
46. Fernandez M, Semela D, Bruix J, Colle I, Pinzani M, Bosch J. Angiogenesis in liver disease. J Hepatol 2009;50:604–620. [PubMed: 19157625]
47. Stetler-Stevenson WG. Matrix metalloproteinases in angiogenesis: a moving target for therapeutic intervention. J Clin Invest 1999;103:1237–1241. [PubMed: 10225966]
48. Theret N, Lehti K, Musso O, Clement B. MMP2 activation by collagen I and concanavalin A in cultured human hepatic stellate cells. Hepatology 1999;30:462–468. [PubMed: 10421655]
49. Wells RG. The role of matrix stiffness in regulating cell behavior. Hepatology 2008;47:1394–1400. [PubMed: 18307210]
50. Fitzgerald KA, Rowe DC, Barnes BJ, Caffrey DR, Visintin A, Latz E, Monks B, et al. LPS-TLR4 signaling to IRF-3/7 and NF-kappaB involves the toll adapters TRAM and TRIF. J Exp Med 2003;198:1043–1055. [PubMed: 14517278]
51. Arras M, Ito WD, Scholz D, Winkler B, Schaper J, Schaper W. Monocyte activation in angiogenesis and collateral growth in the rabbit hindlimb. J Clin Invest 1998;101:40–50. [PubMed: 9421464]

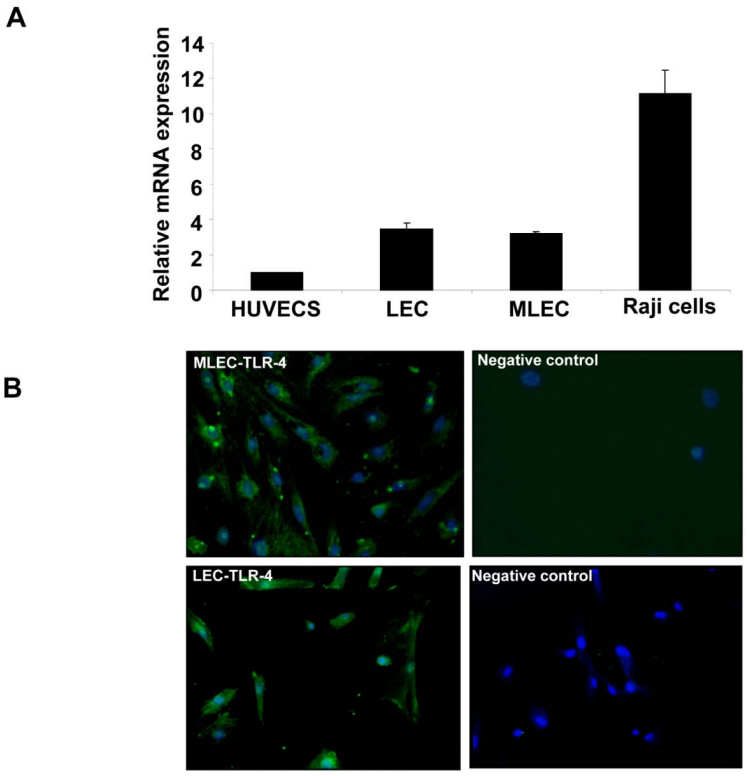

Figure 1. TLR4 is expressed in human and murine LEC

A. Expression of TLR4 cDNA from HUVEC, human and murine LEC and Raji cells amplified using quantitative RT-PCR to measure levels of various TLR. B. Murine and human LEC were isolated and immunostained for TLR4 (green) along with a nuclear counterstain (Blue, DAPI).

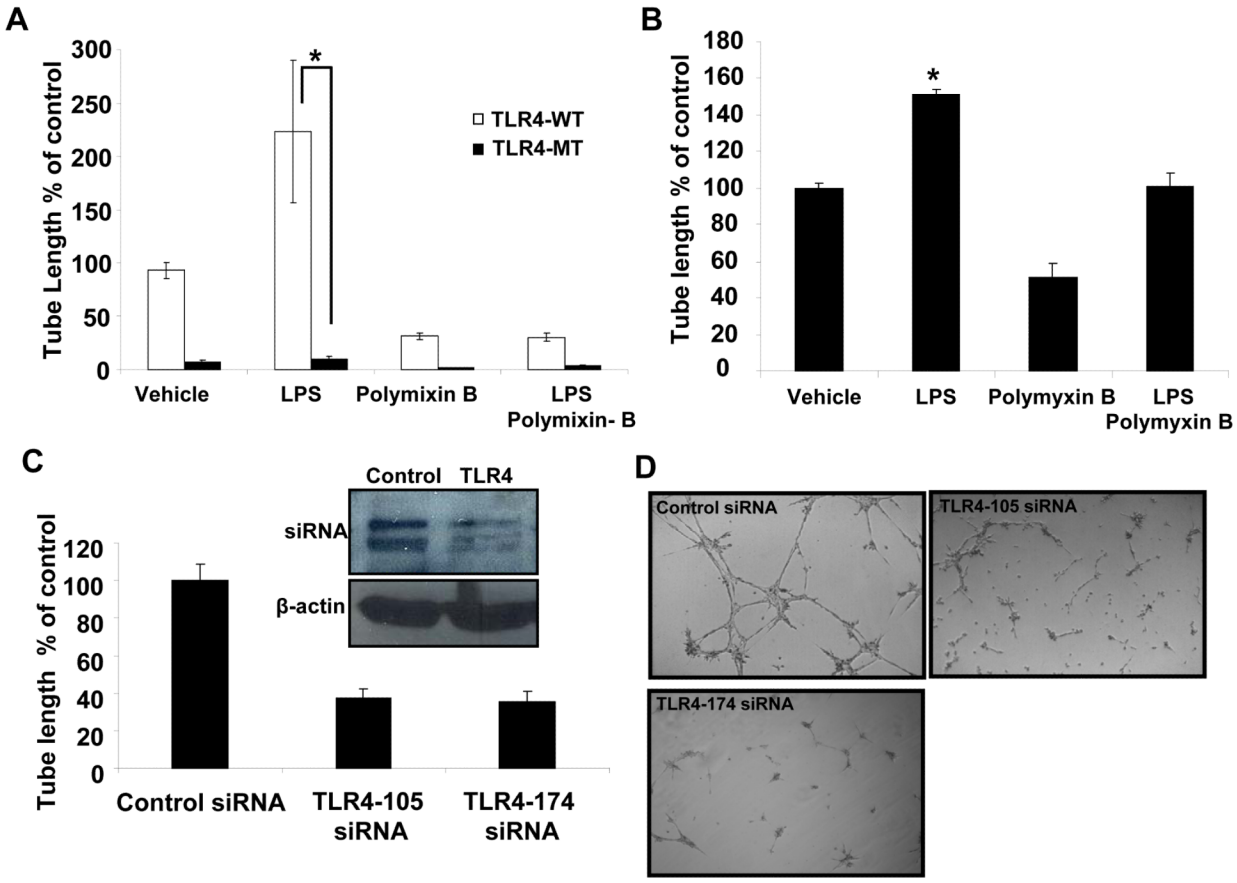

Figure 2. LPS induced tube formation is reduced in TLR4-MT LEC

LEC were isolated from TLR4-WT and TLR4-MT mice and plated on Matrigel. A. Quantification of tubulogenesis stimulated with LPS (1 μg/ml) and/or polymixin B (3 μg/ml) is shown (N=4; mean ± SEM; * indicates P<0.05 vs TLR4-WT). B. Human LEC were stimulated with LPS (1 μg/ml) and/or polymixin B (3 μg/ml) and assessed for tubulogenesis and quantified using Image Pro software (N= 4; mean ± SEM; * indicates P<0.005). C. Quantification of tubulogenesis in human LEC transfected with two distinct TLR4 specific siRNA (N=4; mean ± SEM; * indicates P<0.005). Inset shows the immunoblot for TLR4 and β-actin (50 μg protein/lane). D. Representative micrographs depicting reduced tube formation in cells transfected with TLR4 specific siRNA.

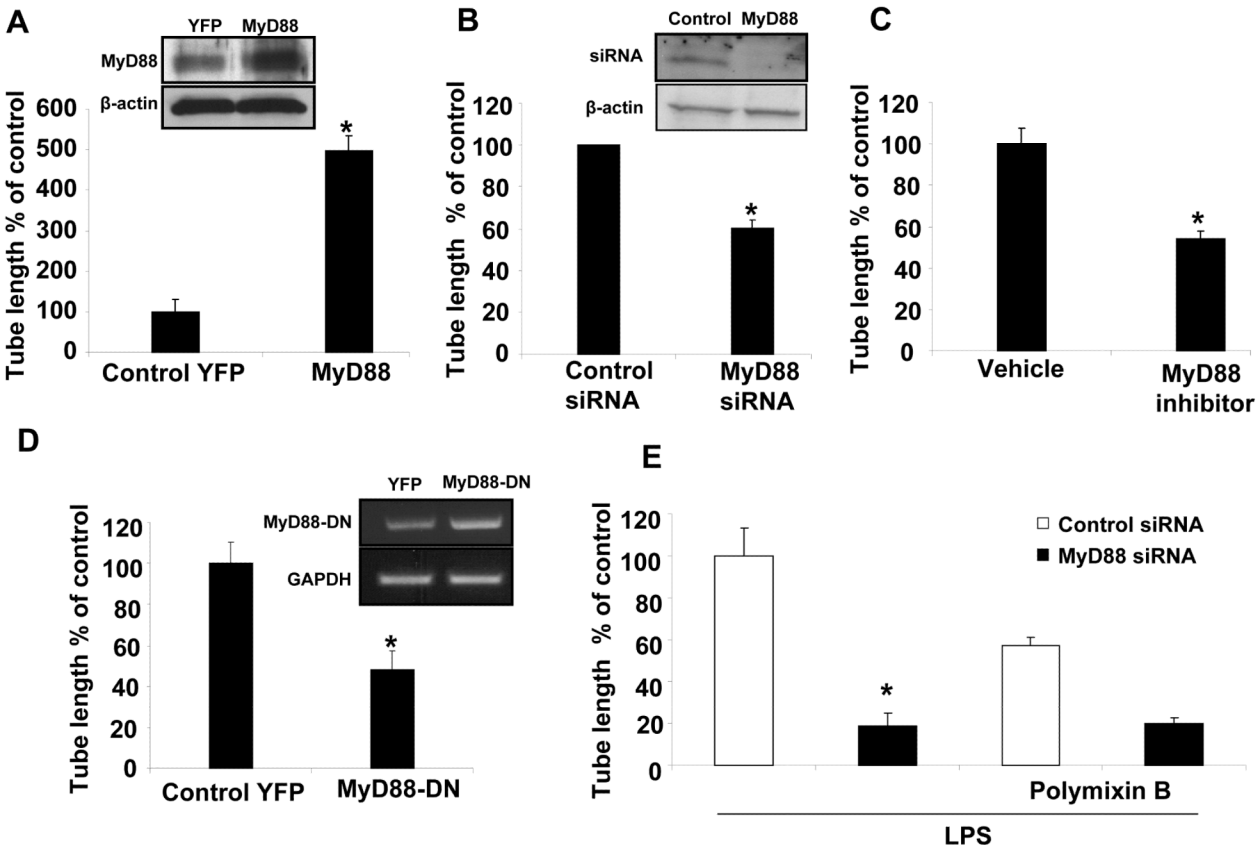

Figure 3. MyD88 regulates TLR4 dependent tubulogenesis

A. Human LEC were transduced with retroviral MyD88 or YFP control and subjected to Matrigel tubulogenesis assay and quantified using Image pro software (N=4; mean ± SEM). Inset Western blot depicts Myd88 overexpression. B. Human LEC were transfected with MyD88 specific siRNA or control siRNA and tubulogenesis was measured (N=3; mean ± SEM). Inset Western blot depicts Myd88 knockdown. C. Human LEC were incubated for 24hrs either with MyD88 inhibitory peptide, IMG-2005-1 (100 μM/mL) or control peptide and tube formation was quantified (N=3; mean ± SEM, * indicates P<0.005). D. Human LEC were transduced with retroviral MyD88-DN or YFP control and tubulogenesis was measured (N=3; mean ± SEM). Inset gel depicts Myd88 dominant negative overexpression by PCR. E. Human LEC were transfected with MyD88 specific siRNA and stimulated with LPS (1 μg/ml) and/or polymixin B (3 μg/ml) and assessed for tubulogenesis and quantified (N= 3; mean ± SEM; * indicates P<0.005).

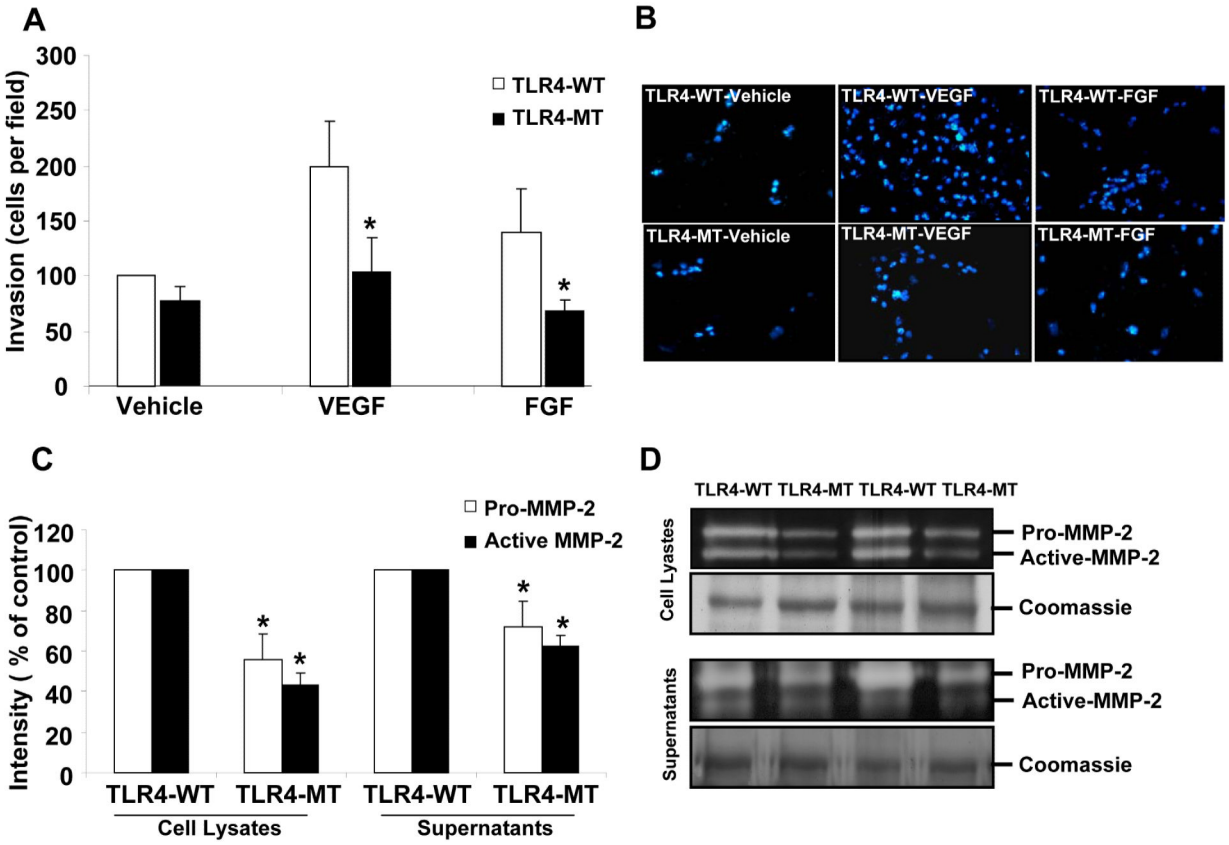

Figure 4. LPS induced matrigel invasion is reduced in TLR4-MT mice

A. Primary LEC were isolated from TLR4-WT and TLR4-MT mice and subjected to 3D collagen invasion assays in the presence or absence of VEGF (10 ng/mL) or FGF (25 ng/mL). Invading cells were stained with DAPI and quantified using Metamorph software (N=5, mean ± SEM; * indicates P<0.03). B. Representative pictures showing reduced invasion in TLR4-MT murine LEC. C. Quantification of gelatinolytic activity using Image-J software is shown (N=3, mean ± SEM; * indicates P<0.05). D. Representative zymogram shows the reduced gelatinolytic activity of MMP-2 in primary TLR4-MT LEC. Representative band from parallel Coomassie stained gel is depicted as a loading control.

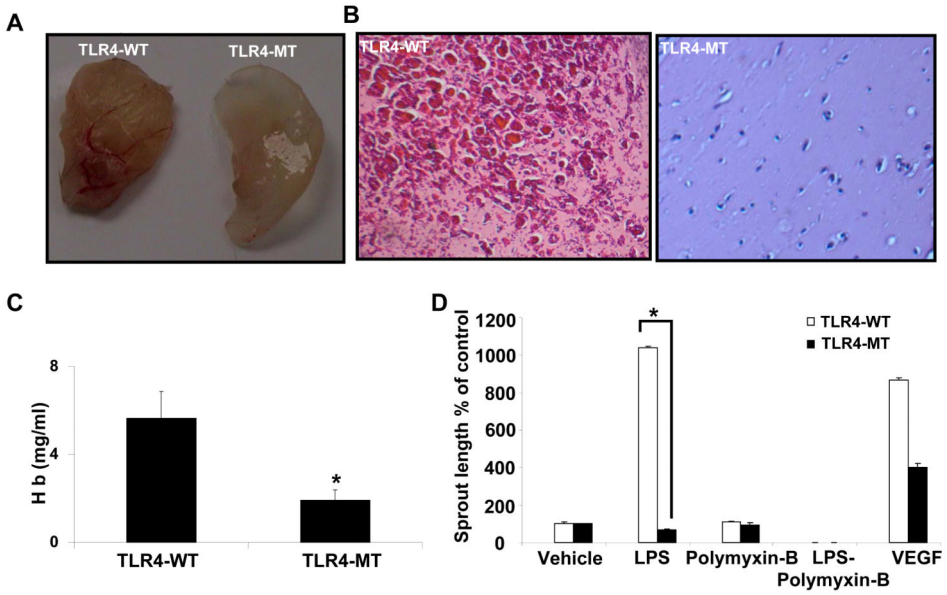

Figure 5. Reduced angiogenesis in TLR4-MT mice

A. TLR4-WT and TLR4-MT mice were implanted with Matrigel subcutaneously for 7 days; representative matrigel explants are shown. B. Paraffin embedded Matrigel explants were H&E stained and representative micrographs are depicted. C. Quantitative analysis of hemoglobin content was normalized to the matrigel explant weight. (N=6-9, mean ± SEM, * indicates $P<0.05$ compared to TLR4-WT). D. Explanted aortic rings were placed on Matrigel and subjected to LPS (1 μg/ml), with or without polymixin B (3 μg/ml), VEGF (10 ng/ml) or complete medium. Histogram shows quantification of aortic sprouts specifically from the endothelial cell lumen; values are represented as arbitrary units (N=4 with 5-6 explants for each mouse, mean ± SEM, * $P<0.05$).

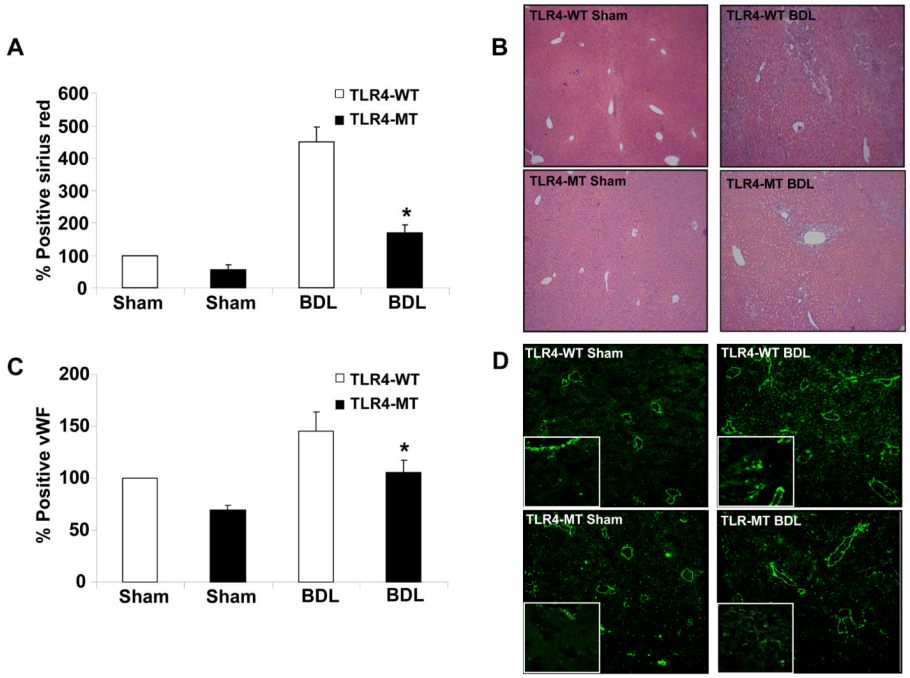

Figure 6. Reduced hepatic vascularization in TLR4-MT compared to TLR4-WT mice in response to liver injury and fibrosis

A. Quantification of fibrosis by Picrosirius red staining in BDL TLR4-WT and TLR4-MT mice. B. Micrographs of representative H&E staining of bile duct ligated TLR4-WT and TLR4-MT mouse liver is depicted. C. Quantification of vWF staining in bile duct ligated TLR4-WT and TLR4-MT mice using Metamorph software is depicted (N=7; mean ± SEM, * indicates P<0.001, TLR4-WT BDL vs TLR4-MT BDL). D. Representative micrographs from each group are depicted; Insets shows 63X magnification of vWF staining LEC from a separate field.

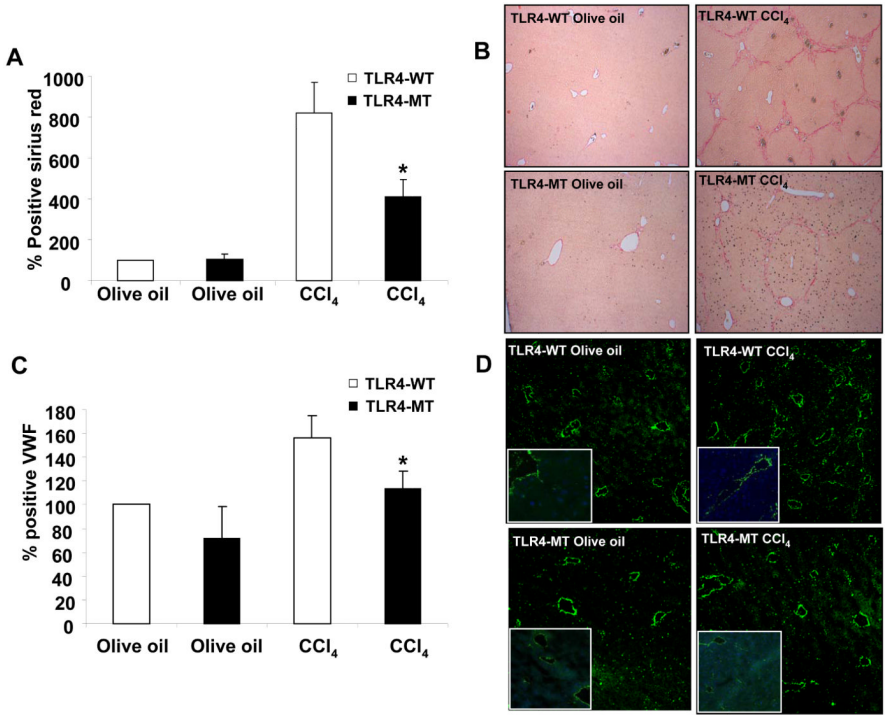

Figure 7. Reduced hepatic vascularization in TLR4-MT compared to TLR4-WT mice in response to CCl_4 induced liver injury and fibrosis

A. Quantification of CCl_4 induced fibrosis by Picrosirius red staining in TLR4-WT and TLR4-MT mice using Metamorph software is depicted. B. Micrographs of representative Picrosirius staining of CCl_4 induced TLR4-WT and TLR4-MT mouse liver is depicted. C. Quantification of vWF staining in CCl_4 induced TLR4-WT and TLR4-MT mice using Metamorph software is depicted (N=6; mean ± SEM, * indicates $P<0.04$, TLR4-WT CCl_4 vs TLR4-MT CCl_4). D. Representative micrographs from each group are depicted; Insets shows 63X magnification of vWF LEC staining from a separate field.